







RESEARCH ARTICLE | FEBRUARY 10 2022

Role of primary and secondary processes in the ultrafast spin dynamics of nickel

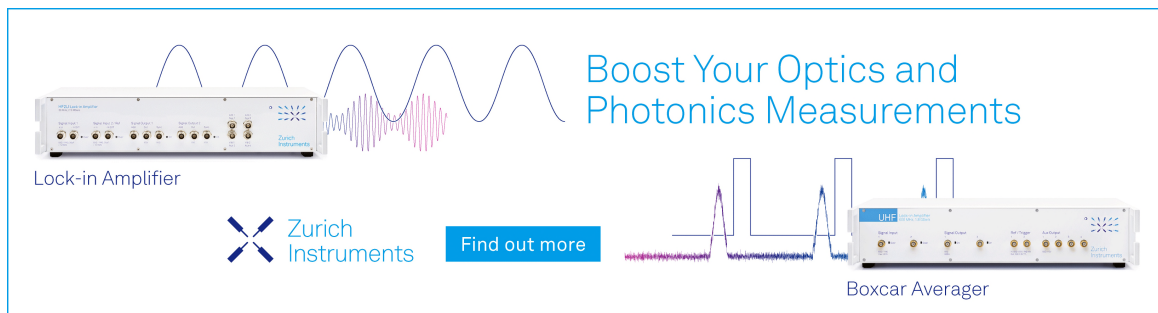
Special Collection: **Ultrafast and Terahertz Spintronics**

Martin Stiehl ; Marius Weber; Christopher Seibel ; Jonas Hofer; Sebastian T. Weber ; Dennis M. Nenno; Hans Christian Schneider ; Baerbel Rethfeld; Benjamin Stadtmüller ; Martin Aeschlimann 



Appl. Phys. Lett. 120, 062410 (2022)

<https://doi.org/10.1063/5.0077213>



Boost Your Optics and Photonics Measurements

Lock-in Amplifier

Zurich Instruments

Find out more

Boxcar Averager

Role of primary and secondary processes in the ultrafast spin dynamics of nickel

Cite as: Appl. Phys. Lett. **120**, 062410 (2022); doi: [10.1063/5.0077213](https://doi.org/10.1063/5.0077213)

Submitted: 31 October 2021 · Accepted: 25 January 2022 ·

Published Online: 10 February 2022



View Online



Export Citation



CrossMark

Martin Stiehl,^{1,a)}  Marius Weber,¹ Christopher Seibel,¹  Jonas Hofer,¹ Sebastian T. Weber,¹  Dennis M. Nenno,¹ Hans Christian Schneider,¹  Baerbel Rethfeld,¹ Benjamin Stadtmüller,^{1,2}  and Martin Aeschlimann¹ 

AFFILIATIONS

¹Department of Physics and Research Center OPTIMAS, University of Kaiserslautern, Erwin-Schroedinger-Strasse 46, 67663 Kaiserslautern, Germany

²Institute of Physics, Johannes Gutenberg University Mainz, Staudingerweg 7, 55128 Mainz, Germany

Note: This paper is part of the APL Special Collection on Ultrafast and Terahertz Spintronics.

^{a)}Author to whom correspondence should be addressed: stiehl@rhrk.uni-kl.de

ABSTRACT

The magnetic response of a ferromagnet after an ultrafast optical excitation can be connected to the underlying electronic dynamics either via primary excitation processes during the laser pulse or via secondary collision processes. In the latter case, the information on the details of the excitation is lost and, therefore, the electron dynamics can be described using quasi-equilibrium concepts. In this work, we study the effect of the pump photon energy on the ultrafast demagnetization dynamics in ferromagnetic nickel. We find that the magnetization dynamics for similar absorbed energies for a range of pump photon energies are almost identical and depend only on the absorbed energy. This is in stark contrast to characteristic differences in the optically excited electronic distributions, as calculated from the band structure. In addition, the measured fluence-dependent dynamics can be reproduced with a model based on local temperatures. These findings indicate that it is mainly secondary processes that are responsible for the observed demagnetization dynamics.

© 2022 Author(s). All article content, except where otherwise noted, is licensed under a Creative Commons Attribution (CC BY) license (<http://creativecommons.org/licenses/by/4.0/>). <https://doi.org/10.1063/5.0077213>

Magnetization dynamics driven by ultrashort optical fields have been studied in a variety of magnetic materials and multilayer structures over the past few decades. Present-day interest of ultrafast magnetization dynamics originated from the pioneering study of optically induced ultrafast demagnetization in ferromagnetic nickel.¹ Beaurepaire and coauthors described the complicated process by a three-temperature model (3TM) in which the magnetic properties are artificially separated into a spin system that is coupled to the “electronic system” (without spin) and the “lattice.” While the 3TM can be useful to reproduce the observed magnetization dynamics, the underlying separation of charge and spin degrees of freedom is phenomenological and the model, therefore, cannot be employed to address a fundamental question that has been around ever since: How is the ultrafast response connected to the dynamics of Bloch electrons with spin? More specifically, one can ask whether the ultrafast dynamics is related to (1) the primary optical excitation process, during which the state of the electrons is determined by the coupling to external fields and cannot be represented in a quasi-equilibrium form, or (2) secondary processes for which the details of the excitation are not

crucial. Importantly, if path 2 applies, the carriers will still be “hot” during the secondary dynamics, which may be due to exchange scattering, spin-flip scattering of the Elliott-Yafet type,^{2–4} or electron-magnon scattering. Figure 1 shows a schematic picture of the different manipulation scenarios using the concepts of the 3TM following the indirect excitation: Path 1 influences the spin/magnetization via a direct path from the optical excitation, whereas path 2 goes through a partial equilibration process of the electrons before the spin/magnetization is changed.

The question concerning the relative importance of path 1 compared to path 2 as discussed above has not been addressed by experiments conclusively. One reason is that most of the time pump pulses from Ti:Sa laser systems operating at 800 nm have been used, which lead to the same wavelength/photon energy dependence of the excited electrons in different experiments. Only recently, comparisons with THz excitation⁵ and different photon energies^{6,7} have started to appear. However, these studies have been performed on sample systems where a possible intrinsic photon energy dependence was superposed by depth-dependent light absorption and nonlocal transport processes.

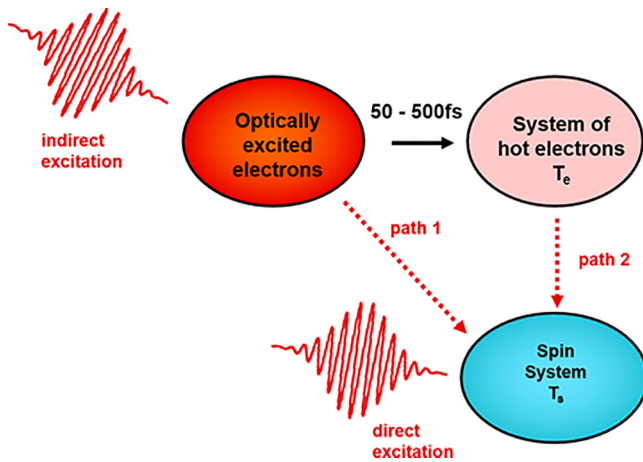


FIG. 1. Schematic picture of local processes after optical excitation using concepts from the 3-temperature model. Path 1 indicates the direct interaction of the optically excited non-equilibrium electrons with the spin system, while path 2 indicates the interaction of the thermalized electrons with the spin system.

In this paper, we aim at distinguishing between the influence of direct primary excitation of the spin system (path 1) and the response of the spins to a system of hot electrons after secondary scattering processes have been at play (path 2). We focus primarily on *local* effects with appropriate sample design, since nonlocal transport processes complicate the dynamics further.^{8–10} In our modeling, we consider incoherent optical excitation based on *ab initio* band structures. We find, however, that the calculated photon energy-dependent differences in the details of absorption do not lead to different experimentally determined magnetization dynamics. Instead, a temperature-based simulation can readily describe the measured tr-MOKE traces. We, therefore, conclude that our results favor path 2 and make path 1 seem unlikely in the sample considered here.

To put our results into perspective, we stress that the focus here is on the distinction between paths 1 and 2, but not on the different theoretical approaches that cover each of these scenarios. For instance, during phase 1, there may be contribution due to *coherent*^{11–14} processes,^{15–17} which generally occur on shorter timescales than the ones considered in this paper. In Fig. 1, this is schematically shown as a direct excitation of the spin system. However, it is also possible that the pulse creates electronic distributions with an imprint of the excitation, which nevertheless can be described by quasi-equilibrium concepts. For instance, differences in the dynamics could occur depending on whether mainly minority or majority carriers are excited. In difference, path 2 could involve a prethermalized state, which is completely determined by the energy deposited by the pump pulse.^{18–22}

The plan of the paper is as follows. We first present a calculation of the electronic distributions that are created by pump pulses of different photon energies. We then discuss the measured magnetization dynamics corresponding to a variety of pump photon energies and compare and contrast these results with the computed optical excitation conditions as well as a simulation of the magnetization dynamics based on local temperatures and chemical potentials.

We determine the effect of the optical pulse on the spin-dependent population of the Ni states from an equation of motion for

the time-dependent distribution functions $n_{\mu\vec{k}}$ for electrons in Bloch states $|\mu\vec{k}\rangle$. We describe the influence of the optical field by diagonal interband transitions $|\mu\vec{k}\rangle \rightarrow |\nu\vec{k}\rangle$ using second-order Fermi's Golden Rule scattering rates,⁴ as described in the [supplementary material](#). In difference to our earlier numerical approach,⁴ the dipole matrix elements and occupation numbers in the ground state are determined by using the ELK DFT code.²³ We assume a Gaussian shaped pulse with a temporal width (full width at half maximum, FWHM) of 50 fs for all photon energies and neglect other scattering processes during the pulse excitation. More details and input parameters for the DFT calculations can be found in the [supplementary material](#).

Figure 2 shows the results of these calculations. In (a), the calculated spin-resolved nickel density of states (DOS) in the ground state is plotted. In Figs. 2(b)–2(d), we show the normalized occupation changes due to the optical excitation for different photon energies. For these three different excitation photon energies, the occupation changes occur at rather well resolved energies, which correspond to the dipole-allowed diagonal transitions in k space. The dominant transitions involve occupied majority spin states from 0.5 eV below the Fermi energy (E_F) in all cases. The minority spin states involved vary in energy. Comparing these energetic regions with the calculated ground state DOS, it is apparent that they correspond to the d-bands of nickel, the, respectively, highest occupied states below E_F for the majority and unoccupied states above for the minority carriers.

Figure 2 demonstrates that the excited carrier distributions for different pump photon energies exhibit some essential differences.

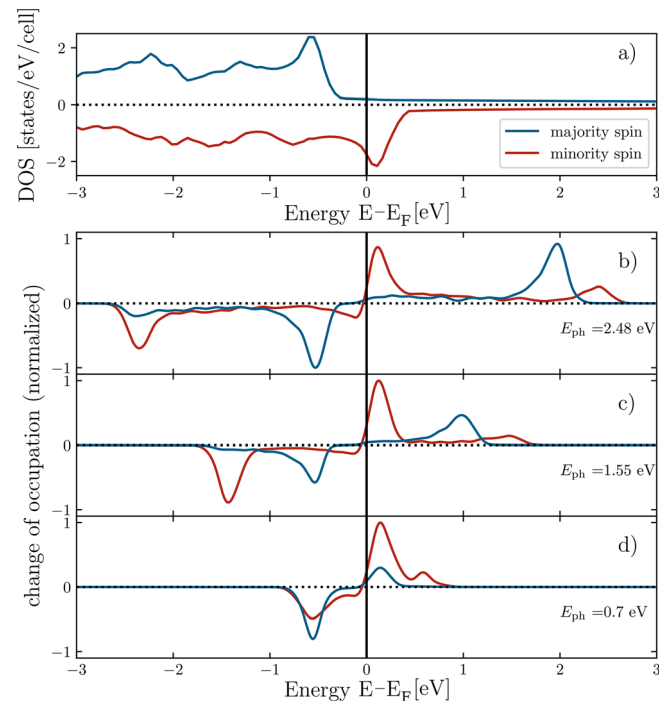


FIG. 2. Calculated ground state DOS of nickel (a) used as a starting point to determine the change in electronic occupation after excitation with (b) 2.48 (500 nm), (c) 1.55 (800 nm), and (d) 0.7 eV (1770 nm) optical pulses. Changes in occupation are normalized to their respective maximum. The energy is given relative to the Fermi energy E_F .

Let us focus on the ratio between excited majority and minority electrons. For 2.48 eV (b), roughly the same density of electrons with both spins is excited, and this ratio is the same for electronic states emptied below E_F . For the photon energy of 1.55 eV (c), more minority electrons are created above E_F and again a similar ratio occurs for emptied electronic states. One notices by inspection that almost no change in the spin polarization due to dipole transitions occurs in Figs. 2(b) and 2(c), and integrating the curves confirms that there is only a few per cent change.

Consider now the photon energy of 0.7 eV where again more minority electron states are populated (as compared to majority electrons) right above E_F . In this case, more *majority* electron states are depopulated so that there are more minority electrons and more majority holes are created,²⁴ and the spin polarization is changed appreciably due to the optical excitation process.⁴ Thus, band structure effects lead to very different distributions of minority and majority carriers. These would be typical primary effects and if they were to influence the magnetization dynamics, it would favor “path 1” in Fig. 1. We have used a completely incoherent calculation of the excited carrier distributions, but it seems likely that if coherent primary effects of the excitation, such as the ones described in Ref. 25, were important, they should also lead to pronounced dependence on the photon energy and, thus, favor “path 1.”

We stress that the photon energy of 0.7 eV is special because it coincides with the exchange splitting of the nickel d-bands and changes in spin polarization result from dipole-allowed transitions between minority and majority states. This behavior occurs for two reasons: First, in the presence of spin-orbit coupling, these states are not pure spin states, which makes it possible for an incoherent transition $|\mu\vec{k}\rangle \rightarrow |\nu\vec{k}\rangle$ to change the admixture of the different spin components in the final and initial states. Second, hybridization of d states with s/p states makes dipole transitions between d-like states possible.

We now turn to an investigation of the magnetization dynamics for a range of photon energies via time-resolved MOKE measurements. Details regarding the experimental setup can be found in the [supplementary material](#). Our studies were performed on a 10 nm polycrystalline nickel film deposited on an insulating MgO substrate in order to exclude transport and exchange-related effects, which compete with the intrinsic photon energy-dependence.^{6,7} To protect the nickel from oxidation and block electrical conductivity, a capping layer of 100 nm Si₂O₃ was deposited on the nickel film from a Si₂O₃ sputtering target without the need for an oxygen atmosphere. The magnetization dynamics on the in-plane magnetized sample were measured using longitudinal MOKE in an all-optical setup. As a probe, we used the second harmonic of our Ti:Sa amplifier with a photon energy of 3.1 eV (400 nm) independent of the applied pump photon energy.

In Fig. 3, we show magnetization traces for selected pump photon energies from the investigated range and carefully chosen pump fluences as described below. All curves exhibit similar magnetization dynamics, which have been measured often for the demagnetization of nickel, following Ref. 1. After the maximum of the laser pulse hits the sample at $t_0 = 0$ ps, a fast drop in the magnetization occurs followed by a comparatively slow remagnetization, which reaches a plateau after approximately 5 ps. The asymptotic behavior on the longer timescales is the result of the electrons (spin) and lattice reaching a thermal equilibrium, a behavior that has been found in electron dynamics calculations^{20,21} and recently has been studied experimentally in some detail,

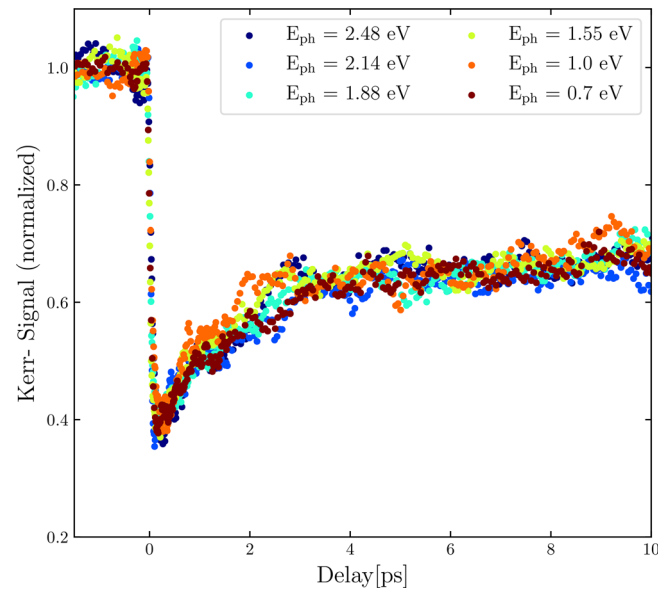


FIG. 3. MOKE traces of the pump induced magnetization dynamics of the 10 nm nickel sample pumped with different pump-photon-energies. The traces shown are chosen to have similar absorbed energies (final magnetization) independent of the pump photon energy.

see, e.g., Ref. 26. The final magnetization and the respective Kerr signal is a monotonous function of the absorbed energy. This dependence allows us to compare magnetization traces for similar absorbed energies for all the used pump photon energies by selecting pump fluences that give rise to magnetization traces with identical Kerr signal at 10 ps delay. These data are displayed in Fig. 3. Using this approach, we do not have to explicitly consider the photon energy dependent absorption efficiency.

We conclude from Fig. 3 the main result of this paper: There are no significant differences in the magnetization dynamics over the whole range of used pump photon energies, *if* one compares the dynamics in cases where the same energy is absorbed by the electron system. Or stated differently, our measurements do not allow us to identify an experimental fingerprint for the different pump photon energies. In more detail, the normalized Kerr signal traces, which are proportional to the magnetization, drop with a demagnetization time of about 40 fs reaching a similar minimum of about 40% of the initial signal followed by nearly parallel remagnetization dynamics with a time constant of approximately 2 ps, reaching similar asymptotic values of about 70%. The deviations between the shown curves can mainly be attributed to deviations in the asymptotic values of the different measurements corresponding to differences in the absorbed energy and small variations in the pulse durations for the different pump photon energies.

If we refer back to Fig. 1, our findings indicate that the magnetization dynamics are not measurably influenced by “path 1.” Rather they are consistent with “path 2,” in which the thermalized electron system, and, therefore, the absorbed energy, plays the dominant role.

The very similar magnetization traces shown in Fig. 3 result from excitation with different pump wavelengths and fluences, but similar absorbed energies. The experimental results suggest that much of the

microscopic detail of the optical excitation is not important for the demagnetization dynamics so that it should be useful to have a macroscopic description of this process. In order to gain an understanding of the observed behavior on such a macroscopic level, we present simulation results from the temperature-based μ T model,²⁷ which we extend by the coupling to substrate phonons. Figure 4 illustrates this model, see the [supplementary material](#) for details. The additional coupling to phonons allows us to consider energy losses to the substrate.²⁸

The results of the temperature-based simulations are shown in Fig. 5 together with measurements for the pump photon energy of 2.21 eV (560 nm) and varying pump fluences. For all fluences, the measurements show a fast drop in the Kerr signal within the first 100 fs representing a demagnetization of the nickel layer. Following this fast drop, the remagnetization occurs within the next few picoseconds, slowing down with increasing absorbed energy. These characteristics of the experiment are qualitatively well reproduced by simulations for different absorbed energies. The simulations also show a fast drop in magnetization, which timescale is mostly independent of the absorbed energy, while the remagnetization also slows down with the increasing absorbed energy. The simulation results are calculated from the absorbed energy and, therefore, do not explicitly include any photon energy dependency. Thus, even though this model does not work with microscopic distribution functions, the good agreement with the experiment suggests that it can describe the magnetization dynamics reasonably well. We interpret this as an indication that for a thin Ni film on an insulating substrate, it suffices to take the absorbed energy into account and neglect the details of the hot electron distribution.

The simulation also yields information about the processes responsible for different parts of the dynamics. The initial drop is caused by the equilibration of temperature and chemical potentials after excitation. The following remagnetization occurs with two steps: first one step on a timescale of a few ps and, second, a longer remagnetization on a timescale of approximately 100 ps. The first and fast remagnetization is caused by energy transfer of the excited electrons to the phonons of the magnetic material, which results in an asymptotic value of magnetization. This value slowly changes on a longer

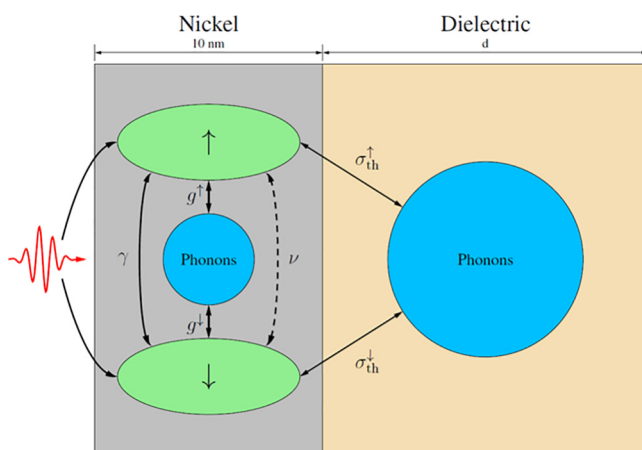


FIG. 4. Interactions taken into account in the μ T model for Ni on an insulating substrate. Solid lines refer to energy exchange, whereas dashed lines refer to particle transfer.

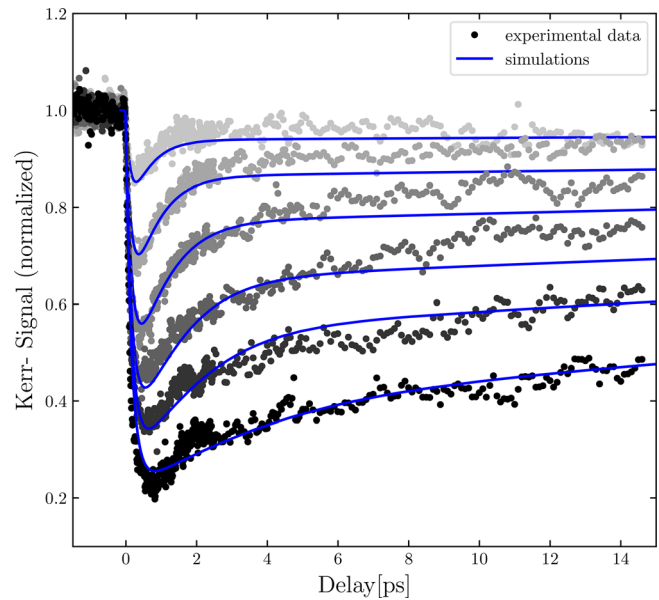


FIG. 5. Measured Ni magnetization traces for pump photon energy of 2.21 eV (560 nm) and various fluences (black dots). Simulated magnetization dynamics obtained from the temperature based μ T model extended by coupling to substrate phonons.

timescale due to the slight energy loss from the nickel layer to the substrate.

In summary, we revisited the problem of how the ultrafast magnetization dynamics can be connected to the underlying electronic dynamics. In particular, we asked whether primary processes during the pulse or secondary processes that can be described by quasi-equilibrium properties are responsible for the observable dynamics. To this end, we studied the influence of optical excitation conditions on ultrafast magnetization dynamics in a ferromagnetic Ni film on an insulating substrate.

We used a time-dependent Fermi's golden rule approach to model the occupation for fixed absorbed energy and found significant differences in the excited electron and hole distributions in the excitation photon energy range from 0.5 to 2.5 eV. In particular, for varying photon energies, we find, apart from dissimilar shapes of the excited carrier distributions, different ratios between the densities of majority and minority carriers.

In order to isolate these differences experimentally, we performed time-resolved MOKE measurements with a thin nickel film on an insulating substrate. We compared measurements of magnetization dynamics obtained with different pump photon energies between 0.7 and 2.48 eV. We chose for comparison magnetization traces for which the same amount of energy had been absorbed in the magnetic film. Contrary to expectations, despite the very different excited electron distributions, the measured tr-MOKE traces were identical.

The shape and fluence dependence of experimental traces could be described well by the temperature-dependent μ T model with a coupling to substrate phonons. These results suggest that the magnetization dynamics are determined by secondary processes, which can be described using quasi-equilibrium concepts, and which are mostly

determined by the absorbed energy. For the given system of a homogeneously heated nickel layer, the details of the excited hot carrier distributions, therefore, seem to have a negligible influence on the ultrafast magnetization dynamics on the considered timescales.

See the [supplementary material](#) that contains detailed information about the density functional theory calculations, including the used input parameters (see Sec. I); the experimental setup (see Sec. II); and the μ T-based calculations, including the used input parameters (see Sec. III).

The authors acknowledge support by the Deutsche Forschungsgemeinschaft (DFG, German Research Foundation) through No. TRR 173–268565370 (project B03). B.S. further acknowledges funding by the Dynamics and Topology Center funded by the State of Rhineland Palatinate.

AUTHOR DECLARATIONS

Conflict of Interest

The authors have no conflicts to disclose.

DATA AVAILABILITY

The data that support the findings of this study are available within the article or are available from the corresponding author upon reasonable request.

REFERENCES

- E. Beaurepaire, J.-C. Merle, A. Daunois, and J.-Y. Bigot, "Ultrafast spin dynamics in ferromagnetic nickel," *Phys. Rev. Lett.* **76**, 4250–4253 (1996).
- B. Koopmans, J. J. Ruigrok, F. Dalla Longa, and W. J. De Jonge, "Unifying ultrafast magnetization dynamics," *Phys. Rev. Lett.* **95**, 267207 (2005).
- K. Carva, M. Battiato, and P. M. Oppeneer, "Ab initio investigation of the Elliott–Yafet electron-phonon mechanism in laser-induced ultrafast demagnetization," *Phys. Rev. Lett.* **107**, 207201 (2011).
- S. Essert and H. C. Schneider, "Electron-phonon scattering dynamics in ferromagnetic metals and their influence on ultrafast demagnetization processes," *Phys. Rev. B* **84**, 224405 (2011).
- A. L. Chekhov, Y. Behovits, J. J. F. Heitz, C. Denker, D. A. Reiss, M. Wolf, and M. Weinelt, "Ultrafast demagnetization of iron induced by optical vs terahertz pulses," [arXiv:2106.01967](https://arxiv.org/abs/2106.01967) (2021).
- U. Bierbrauer, S. T. Weber, D. Schummer, M. Barkowski, A.-K. Mahro, S. Mathias, H. C. Schneider, B. Stadtmüller, M. Aeschlimann, and B. Rethfeld, "Ultrafast magnetization dynamics in nickel: Impact of pump photon energy," *J. Phys.: Condens. Matter* **29**, 244002 (2017).
- V. Cardin, T. Balciunas, K. Légaré, A. Baltuska, H. Ibrahim, E. Jal, B. Vodungbo, N. Jaouen, C. Varin, J. Lüning, and F. Légaré, "Wavelength scaling of ultrafast demagnetization in Co/Pt multilayers," *Phys. Rev. B* **101**, 054430 (2020).
- M. Battiato, K. Carva, and P. M. Oppeneer, "Theory of laser-induced ultrafast superdiffusive spin transport in layered heterostructures," *Phys. Rev. B* **86**, 024404 (2012).
- A. Eschenlohr, M. Battiato, P. Maldonado, N. Pontius, T. Kachel, K. Hollnick, R. Mitzner, A. Föhlich, P. M. Oppeneer, and C. Stamm, "Ultrafast spin transport as key to femtosecond demagnetization," *Nat. Mater.* **12**, 332–336 (2013).
- E. Turgut, C. La-O-Vorakiat, J. M. Shaw, P. Grychtol, H. T. Nembach, D. Rudolf, R. Adam, M. Aeschlimann, C. M. Schneider, T. J. Silva, M. M. Murnane, H. C. Kapteyn, S. Mathias, and P. Gru, "Controlling the competition between optically induced ultrafast spin-flip scattering and spin transport in magnetic multilayers," *Phys. Rev. Lett.* **110**, 197201 (2013).
- These were recently found to be important in the optical spin intersite transfer process (OISTR) in alloys.
- J. K. Dewhurst, P. Elliott, S. Shallcross, E. K. Gross, and S. Sharma, "Laser-induced intersite spin transfer," *Nano Lett.* **18**, 1842–1848 (2018).
- F. Siegrist, J. A. Gessner, M. Ossiander, C. Denker, Y.-P. Chang, M. C. Schroder, A. Guggenmos, Y. Cui, J. Walowski, and U. Martens *et al.*, "Light-wave dynamic control of magnetism," *Nature* **571**, 240–244 (2019).
- M. Hofherr, S. Hauser, J. K. Dewhurst, P. Tengdin, S. Sakshath, H. T. Nembach, S. T. Weber, J. M. Shaw, T. J. Silva, H. C. Kapteyn, M. Cinchetti, B. Rethfeld, M. M. Murnane, D. Steil, B. Stadtmüller, S. Sharma, M. Aeschlimann, and S. Mathias, "Ultrafast optically induced spin transfer in ferromagnetic alloys," *Sci. Adv.* **6**, eaay8717 (2020).
- G. P. Zhang and W. Hübner, "Laser-induced ultrafast demagnetization in ferromagnetic metals," *Phys. Rev. Lett.* **85**, 3025–3028 (2000).
- W. Töws and G. M. Pastor, "Many-body theory of ultrafast demagnetization and angular momentum transfer in ferromagnetic transition metals," *Phys. Rev. Lett.* **115**, 217204 (2015).
- V. Shokeen, M. Sanchez Piaia, J.-Y. Bigot, T. Müller, P. Elliott, J. Dewhurst, S. Sharma, and E. Gross, "Spin flips versus spin transport in nonthermal electrons excited by ultrashort optical pulses in transition metals," *Phys. Rev. Lett.* **119**, 107203 (2017).
- B. Koopmans, G. Malinowski, F. Dalla Longa, D. Steiauf, M. Fähnle, T. Roth, M. Cinchetti, and M. Aeschlimann, "Explaining the paradoxical diversity of ultrafast laser-induced demagnetization," *Nat. Mater.* **9**, 259–265 (2010).
- U. Atxitia, O. Chubykalo-Fesenko, J. Walowski, A. Mann, and M. Münzenberg, "Evidence for thermal mechanisms in laser-induced femtosecond spin dynamics," *Phys. Rev. B* **81**, 174401 (2010).
- M. Krauß, T. Roth, S. Alebrand, D. Steil, M. Cinchetti, M. Aeschlimann, and H. C. Schneider, "Ultrafast demagnetization of ferromagnetic transition metals: The role of the Coulomb interaction," *Phys. Rev. B* **80**, 180407 (2009).
- B. Y. Mueller, A. Baral, S. Vollmar, M. Cinchetti, M. Aeschlimann, H. C. Schneider, and B. Rethfeld, "Feedback effect during ultrafast demagnetization dynamics in ferromagnets," *Phys. Rev. Lett.* **111**, 167204 (2013).
- A. Manchon, Q. Li, L. Xu, and S. Zhang, "Theory of laser-induced demagnetization at high temperatures," *Phys. Rev. B* **85**, 064408 (2012).
- See <http://elk.sourceforge.net/> "The Elk Code."
- In Fig. 2(d), we have an excited-electron spin polarization of 0.63.
- J. K. Dewhurst, S. Shallcross, P. Elliott, S. Eisebitt, C. v. K. Schmising, and S. Sharma, "Angular momentum redistribution in laser-induced demagnetization," *Phys. Rev. B* **104**, 054438 (2021).
- M. Hofherr, S. Moretti, J. Shim, S. Häuser, N. Y. Safonova, M. Stiehl, A. Ali, S. Sakshath, J. W. Kim, D. H. Kim, H. J. Kim, J. I. Hong, H. C. Kapteyn, M. M. Murnane, M. Cinchetti, D. Steil, S. Mathias, B. Stadtmüller, M. Albrecht, D. E. Kim, U. Nowak, and M. Aeschlimann, "Induced versus intrinsic magnetic moments in ultrafast magnetization dynamics," *Phys. Rev. B* **98**, 174419 (2018).
- B. Y. Mueller and B. Rethfeld, "Thermodynamic μ T model of ultrafast magnetization dynamics," *Phys. Rev. B* **90**, 144420 (2014).
- K. Sokolowski-Tinten, X. Shen, Q. Zheng, T. Chase, R. Coffee, M. Jerman, R. K. Li, M. Ligges, I. Makasyuk, M. Mo, A. H. Reid, B. Rethfeld, T. Vecchione, S. P. Weathersby, H. A. Dürr, and X. J. Wang, "Electron-lattice energy relaxation in laser-excited thin-film Au-insulator heterostructures studied by ultrafast MeV electron diffraction," *Struct. Dyn.* **4**, 054501 (2017).